Analytica Chimica Acta 1038 (2018) 173–181

Contents lists available at ScienceDirect

Analytica Chimica Acta

journal homepage: www.elsevier.com/locate/aca

Non-SELEX isolation of DNA aptamers for the homogeneous-phase fluorescence anisotropy sensing of tau Proteins

Samuele Lisi [a, b], Emmanuelle Fiore [a], Simona Scarano [b], Emanuela Pascale [b], Yannik Boehman [c], Frederic Ducongé [d], Sabine Chierici [e], Maria Minunni [b], Eric Peyrin [a, **], Corinne Ravelet [a, *]

[a] Univ. Grenoble Alpes, DPM UMR 5063, CNRS, F-38041 Grenoble, France
[b] Department of Chemistry 'Ugo Schiff', Via della Lastruccia 3-13, Sesto Fiorentino, 50019, Firenze, Italy
[c] Unité des virus émergents, UMR IRD 190 EPV, Faculté de Médecine-Timone, 27 boulevard Jean-Moulin, 13385 Marseille Cedex 5, France
[d] CEA, Fundamental Research Division (DRF), Institute of Biology François Jacob (Jacob), Molecular Imaging Research Center, Neurodegenerative Diseases Laboratory, CNRS UMR 9199, Paris-Saclay University, Fontenay aux Roses, France
[e] Univ. Grenoble Alpes, DCM UMR 5250, CNRS, F-38041 Grenoble, France

HIGHLIGHTS

- A new DNA aptamer against Alzheimer's disease biomarkers (τ-441, τ-381, τ-352 and τ-383) was selected.
- Non-SELEX was used to isolate high-affinity DNA sequences in one working day.
- The affinity constants were comparable with those previously reported for CE-SELEX-selected aptamers.
- A fluorescence anisotropy sensing platform allowed the detection of the four τ-isoforms with a nM detection limit..

GRAPHICAL ABSTRACT

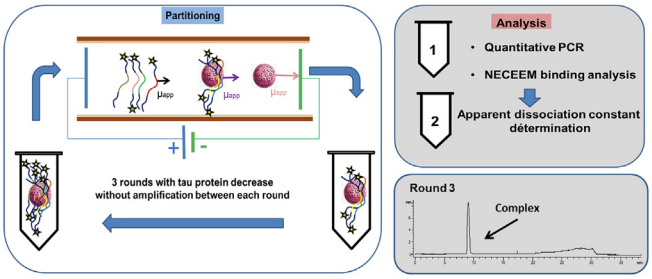

ARTICLE INFO

Article history:
Received 11 February 2018
Received in revised form
9 July 2018
Accepted 13 July 2018
Available online 17 July 2018

Keywords:
Alzheimer disease
Tau protein
Aptamer
SELEX
Fluorescence anisotropy

ABSTRACT

Herein, we report for the first time the isolation of DNA aptamers directed against the whole tau protein, an important Alzheimer's disease (AD) biomarker. Non-SELEX approach based on the capillary electrophoresis partitioning technique was employed to isolate a high-affinity DNA sequence pool towards the target in only three rounds and one working day. High-throughput sequencing was next performed and the recognition ability of five selected aptamers was preliminary evaluated by surface plasmon resonance using the protein target immobilized on the chip. Finally, the analytical potential of the most affine aptamer was demonstrated through the design of a homogeneous-phase fluorescence anisotropy assay. This DNA aptamer was found to be able to recognize not only the whole τ-441 but also the τ-381, τ-352, τ-383 isoforms. The sensing platform allowed the determination of these four targets with a detection limit of 28 nM, 3.2 nM, 6.3 nM and 22 nM, respectively.

1. Introduction

The most accepted biomarkers currently used in the aid for the AD diagnosis are the cerebrospinal fluid (CSF) amyloid beta

* Corresponding author.
** Corresponding author.
E-mail addresses: eric.peyrin@univ-grenoble-alpes.fr (E. Peyrin), corinne.ravelet@ujf-grenoble.fr (C. Ravelet).

https://doi.org/10.1016/j.aca.2018.07.029
0003-2670/

peptides (Ab1-42 and Ab1-40), tau protein phosphorylated on threonine 181 (p-τ 181), and total tau protein which represents the six isoforms (t-τ) [1].

Numerous analytical methods have been described to detect these AD markers in the biological fluid of election, i.e. CSF. The established approaches are based on the immunoassay principles with a variety of signaling techniques ranging from conventional ELISA-derived systems to emerging sensing platforms based on electrochemical, optical, and piezoelectric transduction [2]. However, immunological methods suffer from a number of drawbacks including the analysis cost [3], the difficulty of standardization and the assay interferences [4]. In this context, recent research efforts have focused on the development of alternative, biomimetic recognition elements such as peptides, molecular imprinting polymers, and nucleic acid aptamers.

While aptamers have stimulated growing interest in both diagnostics and therapy, up to now only a few works have been performed in the development of functional oligonucleotides specific to AD markers [5]. The reported aptamers mainly target the Ab peptides whereas only one aptamer has been described for the longest isoform of human τ protein. Indeed, on the basis of the well-known ability of τ protein to interact with RNA molecules [6], Kim and colleagues reported a 12-round SELEX for isolating RNA sequences (K_D in the 40–200 nM range) that are notably able to inhibit the τ oligomerization propensity [7]. However, the analytical potential of these SELEX-isolated sequences has not been yet demonstrated. Furthermore, DNA aptamers would be more desirable than RNA aptamers in terms of both biostability and cost of synthesis. The only nucleic acid sensing platform dedicated to the τ-381 detection reported up to now is based on a combined DNA-antibody sandwich assay [8] using surface plasmon resonance (SPR) technology. Nonetheless, contrary to what was stated by the authors [8], the single-stranded (ss) DNA employed as the capture element in the analytical device cannot be considered as an aptamer (that is, selected from a large pool of random sequences) because it was identified from only three arbitrarily chosen oligonucleotides. Moreover, although one ssDNA strand exhibited a high nanomolar dissociation constant (in the 190–350 nM range for τ-381 and τ-410 respectively), the two other sequences displayed weak-to-very weak affinities [9,10]. Finally, despite its sensitivity, the heterogeneous-phase nature of the SPR technique requires the careful control of the surface chemistry for the molecule attachment to the chip in order to limit non-specific interactions as well as possible detrimental effects on the recognition features of the capture element [7].

Among SELEX methodologies, capillary electrophoresis-based SELEX (CE-SELEX) [11–13] presents some significant advantages, such as very low sample consumption and no need of both target immobilization and negative selection steps [11]. This technique is very well adapted to peptide or protein binding DNA aptamers selection without target modification, as recently demonstrated for the αC-conotoxin PrXA target, a marine snail ultra-fast-killing paralytic toxin [14]. A modified version of CE-SELEX, named non-SELEX, has been subsequently reported by Krylov and co-workers. While in conventional CE-SELEX each round is followed by Polymerase Chain Reaction (PCR) amplification, selection cycles in non-SELEX are carried out without amplification steps between them, speeding-up the selection process and alleviating the emergence of byproducts sequences [15]. Despite the above-mentioned advantages, only very few examples of aptamer isolation by non-SELEX have been yet reported by capillary electrophoresis [16,17] or with other methods such as PVDF membrane with only one round of selection [18].

In this work, we aimed at identifying DNA aptamers by a fast non-SELEX strategy in order to design a fluorescence anisotropy (FA) aptasensing platform for the τ detection. The signaling fluorescence anisotropy technique displays several advantageous features including its homogeneous-phase nature, simplicity, rapidity, and reliability [19]. The selection of aptamers was performed by a non-SELEX approach starting from a library of 5.10^{12} DNA sequences. High-affinity sequences for the τ-441 target were identified in only 3 rounds and one working day. After high-throughput sequencing, surface plasmon resonance [20] was used to assess the recognition ability of five selected DNA aptamers. Finally, the analytical potential of the best performing aptamer was established through the development of a FA aptasensor dedicated to four isoforms of the τ protein (τ-441, τ-381,τ-352 and τ-383).

2. Experimental section

2.1. Materials

The longest human tau protein isoform (τ-441) was purchased from Enzo Life Science (Lyon, France), supplied lyophilized and reconstituted as recommended by the seller. The τ protein isoforms (τ-381, τ-352 and τ-383) were obtained from Abcam (Cambridge, UK). Human Serum Albumin (HSA), mesityloxide (MO), trizma base (tris), glycine (gly) and all the reagents for acrylamide gel preparation were purchased from Sigma Aldrich (St Quentin Fallavier, France). N-hydroxysuccinimide (NHS) was from Fluka (Milan, Italy); sodium acetate and glycerol were from Carlo Erba reagents (Milan, Italy); 1-ethyl-3-(dimethylaminopropyl) carbodiimide (EDAC) was from Merck (Darmstadt, Germany); 4-(2-hydroxyethyl) piperazine-1-ethanesulfonic acid (HEPES), ethylenediaminetetraacetic acid (EDTA), ethanolamine hydrochloride (EA) used for SPR experiments were all from Sigma Aldrich (Milan, Italy). Other chemicals for buffer preparation were commercially available and purified at analytical grade. The 77-nucleotide fluorescently labeled single-stranded DNA (ssDNA) library and the primers used in this study are presented in Table S1. Heavier reverse primer, and reverse primer were from Eurofins Genomics (Ebersberg, Germany). ssDNA library, labeled (5′-FAM-) and unlabeled forward primer were from Eurogentec (Liege, Belgium). GeneAmp 10X PCR buffer II, AmpliTaq Gold DNA polymerase and SYBR® green PCR Kit were provided from Applied Biosystems (Foster city, California, USA).

2.2. Procedure for R3 peptide synthesis

R3 peptide derivative was synthesized in the DCM laboratory. Assembly of the protected R3 peptide (Ac-GGGKVQIVYKPVDLSKVTSKCG-$CONH_2$) was carried out automatically on an ABI 433 synthesizer (Applied Biosystems) by solid-phase peptide synthesis using the standard 9-fluorenylmethoxycarbonyl/tertiobutyl protection strategy on the rink amide MBHA resin (Novabiochem®). Coupling reactions were performed in NMP using DIPEA as base and HBTU dissolved in DMF as coupling agent. Finally, Boc-protected aminooxyacetic acid was coupled at the *N*-terminus and the peptide was cleaved from the resin using a mixture of TFA/TIS/H_2O (95:2.5:2.5). The cleaving mixture was concentrated under vacuum and the crude was reacted with acetone. After evaporation of the solvent, the peptide was precipitated in diethyl ether. It was purified by RP-HPLC on a Nucleosil C18 column (100 Å, 250 × 21 mm, 7 μm) with UV monitoring at 214 nm and 250 nm at a 20 mL min^{-1} flow linear gradient of 5–60% acetonitrile in water over 30 min (both water and acetonitrile contained 0.1% TFA). After lyophilisation, the R3 peptide was analyzed by electrospray mass spectroscopy: ESI (+) *m/z* 1188.8 (m/2), 792.9 (m/3), 595.0 (m/4).

2.3. Non-SELEX procedure

Capillary electrophoresis selection was performed using a Beckman Coulter P/ACE MDQ system (Fullerton, California, USA) with exchangeable UV absorbance and laser-induced fluorescence (LIF) detectors (λ_{ex} 488 nm and λ_{em} 520 nm) equipped with an 80 cm total length (70 cm effective length) fused silica capillary (Polymicro Technologies Inc., Phoenix, Arizona, USA) and 75 μm inner diameter. Prior to the sample injection, the capillary was conditioned through the following washing steps at 20 psi: 1 M NaOH for 5 min, water for 5 min and migration buffer (50 mM Tris, pH 8.34) for 30 min. Further washing process was performed between each run at 20 psi with 1 M NaOH (2 min), water (2 min) and migration buffer (5 min) to improve repeatability of peak migration time. The voltage applied during separation was 20 kV for all experiments.

Before selection, a 40 μM ssDNA library was heated to 80 °C for 5 min in 4X binding buffer (final concentrations: 10 mM Tris, 20 mM NaCl, 1 mM $MgCl_2$; pH 8.34) and left at room temperature for 10 min. The τ protein was then added to the library to a final concentration of 7.50 μM for the first round of selection, 750 nM and 75 nM for rounds 2 and 3, respectively. The ssDNA library was allowed to incubate with the τ protein at room temperature for at least 20 min to ensure that the binding reached equilibrium. The equilibrated sample was injected by applying 0.7 psi to the capillary inlet for 40 s and detected using UV at 200 nm to monitor the separation. Approximately 209 nL of 40 μM of DNA library (around 8.10^{12} mol) were injected into the capillary during the first selection round, corresponding to almost 5.10^{12} sequences. During a selection round, the eluate was collected into 30 μL of migration buffer until the unbound DNA began to elute. Subsequent rounds of selection used the collected DNA fraction from the previous round as the input DNA. Immediately after migration, the collected mixture was incubated with a new aliquot of the target (until a final volume of 40 μL) and injected again for the new selection cycle.

Quantitative PCR experiments (q-PCR) were carried out on collecting samples, issued from CE separation, to first determine suitable target concentration to begin the selection and second to follow sequence number. Experiments were carried out on Applied Biosystem StepOne™ qPCR instrument (Applied Biosystem, Foster city, California, USA) following the previously published protocol [21]. Briefly, 2 μL of collected ssDNA were mixed with 18 μL of SYBR® green PCR Kit (final volume 20 μL). The final concentration of forward primer and reverse primer were kept at 10^{-6} M final concentration. Thermal cycle consisted in initial denaturation at 95 °C (10 min), followed by 36 amplification cycles during 15 s at 90 °C were alternated with 30 s annealing/extending step at 60 °C. Threshold cycles (C_t) were determined for each round of selection.

2.4. PCR amplification and purification of sequences by gel electrophoresis

Single-stranded DNA candidates were generated by PCR using a reverse primer and a 5′-FAM-labeled forward primer at the end of the selection procedure. The reverse primer is made heavier with a succession of six C_3 links extended with a 5′ DNA stretch of 20 nucleotides. During PCR, this six C3 region and the 20-nucleotide stretch cannot be amplified by the Taq DNA polymerase. A PCR product with two strands of unequal length is consequently synthesized. Each strand is then easily purified on a denaturing polyacrylamide gel. All PCRs were performed using a Biometra cycler from Labgene (Archamps, France). Master mix was made by combining 623 μL nuclease-free water, 32 μL deoxyribonucleotide triphosphate (dNTPs) (25 mM of each) (Invitrogen, Cergy-Pontoise, France), 10 μL each of forward and heavier reverse primers (10^{-4} M), 120 μL $MgCl_2$ (25 mM), and 100 μL GeneAmp 10X PCR buffer II. After mixing, 5 μL (5 U μL^{-1}) of the AmpliTaq Gold DNA polymerase were added. To finish, 100 μL of DNA collected during selection were added. This mixed solution was divided equally over ten thin-walled tubes that were subjected to PCR. The thermal cycling regime was as follows: initial denaturation for 10 min at 95 °C, and then cycling for 60 s at 95 °C, 60 s at 60 °C and 90 s at 72 °C for 14 cycles. After a Nanosep® 3 K purification (Pall, Washington, New York, USA), the samples, which contained different amounts of amplified products, were resolved on a 12% acrylamide gel at an applied voltage of 300 V. The band corresponding to the selected aptamers migrated with the same velocity of the library (used as a witness) and was visualized by UV-shadow method at 254 nm. After that, it was cut and eluted for 1 h at 65 °C and 1 h at 4 °C, in 1 mL of the extraction buffer (100 mM Tris-HCl, 500 mM NaCl, 1 mM EDTA; pH 7.4). To remove acrylamide, the extracted product was transferred into a Nanosep® 3 K device, the retention membrane was replaced by glass wool and the system was centrifuged during 10 min at 14,000 rpm with MIKRO 220R centrifuge (r = 87 mm) (Hettic centrifuges, Tuttlingen, Germany). Filtrate was removed, transferred in another native Nanosep® 3 K device and centrifuged for 90 min at 5000 rpm at 15 °C. The material retained on the top of the porous membrane was washed with 100 μL of water and centrifuged again. Finally, ssDNA amount for each round was quantified by UV absorbance at 260 nm for binding affinity analysis of DNA pools. Three rounds of selection were performed, and the progress of selection was monitored using NECEEM to estimate the bulk affinity.

2.5. Monitoring of the non-SELEX progress

2.5.1. NECEEM-based measurement

CE separation and incubation buffer conditions were identical to those used during the non-SELEX process. Equilibrium mixture was composed of 100 nM 5′-FAM-ssDNA (original library or purified selected pools after PCR amplification) and τ protein (3 μM) incubated for 30 min. Samples were prepared as previously seen and were injected by applying 0.7 psi pressure at the inlet of the capillary for 20 s. Detection of species was insured by LIF detector. K_D values for τ–aptamer interaction were calculated from NECEEM electropherograms as described in details elsewhere [22].

2.6. High-throughput sequencing

After 3 rounds of the non-SELEX procedure, an aliquot of the library was PCR-amplified under the same conditions described previously, except using unlabeled forward primer and free reverse primer (Table S1). The double-stranded DNA PCR product was then purified with MinElute PCR Purification Kit Qiagen (70 bp to 4 kb) and eluted in very small volumes (10 μL). Next Generation Sequencing (NGS) was used to determine aptamer sequences. According to the protocol, DNA concentrations were adjusted to 200 nM (Qubit® dsDNA BR Assay Kit and Qubit® 2.0 Fluorometer) and a library was built using AB Library Builder System and Ion Xpress Barcode. Clonal amplification was performed using the Ion One Touch 2 system and the Ion PGM Template OT2 200 kit (all materials were from Life Technologies SAS, Saint Aubain, France).

The sequencing step was performed using the Ion PGM™ Sequencing 200 Kit v2, the Ion 316 Chip and the PGM instrument, Personal Genome Machine (PGM™) System (Life Technologies SAS, Saint Aubin, France). The PGM technology is based on the detection of releasing hydrogen ion during nucleotide incorporation in DNA template sequences [23]. In case of all chip micro-wells, the incorporated dNTP and the release of a proton triggers an ion sensor and an electrical signal indicates that a reaction has occurred. Automated

read datasets were provided by Ion Torrent software 7.0.3 as FASTQ format. Sequences were then processed using a software suite named PATTERNITY-SEQ developed from the plateform aptamer in MIRcen (http://www.cea.fr/drf/ifrancoisjacob/Pages/Departements/MIRCen/Plateformes.aspx?Type=Chapitre&numero=6).

Sequences corresponding to the variable region between the primer sequences were recovered. Sequences that contain at least one base with a quality score (Q) below 30 were removed before further analysis, it means that the recovered sequences contain bases with a potential probability of error below 0.001 (1 in 1000). These sequences were then saved in a fasta format and the frequency of each sequence in the library was calculated. All sequences were then compared to each other using the Levenshtein distance in order to cluster them in families [24]. Enrichment of sequence motifs were searched in the sequences of 29 and 30 nucleotides using MEME (Multiple Em for Motif Elicitation, where Em stand for the algorithm used for motif discovery) [25].

2.7. Evaluation of selected aptamers by SPR

BIAcore X™ apparatus (GE Healthcare, Uppsala, Sweden) was used for all experiments. τ protein was immobilized on a CM5 sensor chips (GE Healthcare, Uppsala, Sweden) by amino-coupling reaction on carboxylated dextran, flowing HBS-EP buffer (10 mM HEPES, 150 mM NaCl, 3 mM EDTA, with 0.005% Tween 20; pH 7.4) as suggested by the supplier. The chip dextran surface was activated by the injection of 50 mM/200 mM solution of NHS/EDAC (10 min, 5 μL min^{-1}), followed by the injection (30 min, 2 μL min^{-1}) of 100 mg L^{-1} τ protein dissolved in 10 mM acetate buffer at proper pH. Optimal conditions were preliminary evaluated by a preconcentration test aimed to identify the best pH value for protein immobilization. In the end, ethanolamine (1 M, pH 8.5) was used to block residual active sites (15 min, 5 μL min^{-1}).

To investigate relative binding abilities of the five selected aptamers, each sequence was separately injected for 5 min in the system at 1 μM, and resulting sensorgrams were analyzed by BIAevaluation 3.1 software. The regeneration of the biochip among injections was carried out with short 20 mM HCl pulses (1–2 min). Measurements were performed in HBS-EP (10 mM HEPES, 150 mM NaCl, 3 mM EDTA, with 0.005% Tween 20; pH 7.4) both as running buffer and for aptamer dilutions. The flow rate was maintained at 5 μL min^{-1} and temperature at 25 °C.

2.8. Fluorescence anisotropy-based measurement

Once the five selected sequences evaluated, the best performing aptamer, *i.e.* the 3146 one, was used as recognition element for the development of FA homogeneous assay. FA measurements were performed to study the binding interaction of aptamer 3146 with the four τ protein isoforms, the R3 peptide and HSA as non-cognate protein. A Tecan Infinite F500 microplates reader (Männedorf, Switzerland) with 96-wells black microplates (Grenier Bio-One, Courtaboeuf, France) was used. The working aptamer solutions were obtained by adequate dilution of the mother solution (10^{-6} M in water) in a 2X oligonucleotide buffer (40 mM Tris HCl pH 7.5 and 4 mM $MgCl_2$). After preparation, the working solutions were heated at 80 °C for 5 min and left to stand at room temperature for 30 min.

50 μg at 0.2 mg ml^{-1} of τ-381, τ-383 and τ-352 in 25% glycerol, 50 mM Tris HCl, pH 7.5, 150 mM NaCl, 0.25 mM DTT and 0.1 mM PMSF were purchased from Abcam. The concentration of the stock solution of τ-381 (5 μM), τ-383 (5 μM), τ-352 (5.4 μM) was determined by using the calculated molecular mass of each isoform (39.7, 40 and 36.8 kDa, respectively). These molecular masses differ from those derived from the supplier SDS-PAGE experiments (54, 52 and 49 kDa, respectively), as SDS molecules do not bind uniformly to all proteins [26]. These stock solutions were diluted 2.5 fold in water. For comparative experiments, the τ-441 isoform at 21.8 μM (using the calculated molecular mass) in 50 mM MES pH 6.8, 100 mM NaCl and 0.5 mM EGTA was diluted with the 2X concentrated target buffer (40 mM Tris, pH 7.5; 120 mM NaCl and 20% glycerol). HSA and R3 peptide at respectively 21.8 μM and 1.48 μM in water were prepared in the same manner. All the target dilutions were prepared with 1X target buffer (20 mM Tris, pH 7.5; 60 mM NaCl and 10% glycerol).

Experiments were then performed in microplates by mixing 20 nM of 5′-FAM-3146 aptamer (22.5 μl) with the same volume of prepared targets protein dilutions. Blank wells of the microplate received 22.5 μL of the 1X oligonucleotide buffer and 22.5 μl of the 1X target buffer in such a way that the buffer was at 20 mM Tris, pH 7.5; 30 mM NaCl, 5% glycerol and 1 mM $MgCl_2$. After mixing, sample solutions were immediately analyzed. Excitation was set up at 485 ± 20 nm and emitted light was collected at 525 ± 25 nm. Experiments were realized in triplicate.

Fluorescence anisotropy was directly calculated by the instrument software, and the signal was expressed as the difference ($\Delta r = r - r_f$) between that obtained in the presence of the target (r) and that of the free fluorescently labeled aptamer (r_f). For studying the binding equilibrium between the τ protein isoforms and aptamer, the fraction of the τ protein-bound aptamer (f_b) is derived from the measured fluorescence anisotropy, as follows [19]:

$$f_b = \frac{\left(r - r_f\right)}{g(r_b - r) + \left(r - r_f\right)} \quad (1)$$

where r_b represent the anisotropy for the τ protein-bound aptamer probe, it was calculated from the model. The g parameter corresponds to the quantum yield enhancement factor, which is derived from the ratio of the total emission intensity (I) of the τ protein-bound aptamer probe (I_b) to that of the free tracer (I_f), *i.e.* I_b/I_f. As frequently observed for DNA-protein associations [27], f_b can be linked to the microscopic dissociation constant of the aptamer-τ protein complex (K_D) and the free concentration of τ protein ([protein]) through the cooperative Hill binding model [28]:

$$f_b = \frac{[\text{protein}]^{n_H}}{(K_D)^{n_H} + [\text{protein}]^{n_H}} \quad (2)$$

where n_H corresponds to the Hill coefficient that determines the degree of binding cooperativity (<1 for noncooperative binding and >1 for positively cooperative binding).

3. Results and discussion

3.1. Non-SELEX isolation of τ-binding DNA sequences

The whole process of the non-SELEX selection was derived from the previous works of Krylov and co-workers and is depicted in Scheme 1. Briefly, the fluorescently labeled nucleic acid library (30 random nucleotides) was incubated with the protein target in the binding buffered solution and a short plug of the equilibrium mixture was injected onto the capillary prefilled with the run buffer. An electric field was applied to provide the separation between the protein-bound DNA and the free DNA library under non-equilibrium conditions. The DNA binder fraction was then collected from the output of the capillary and subsequently equilibrated with the target for another CE-based partitioning step. The procedure was repeated two more times (a total of 3 rounds) and the third enriched DNA pool was finally PCR amplified for analysis by high-throughput sequencing.

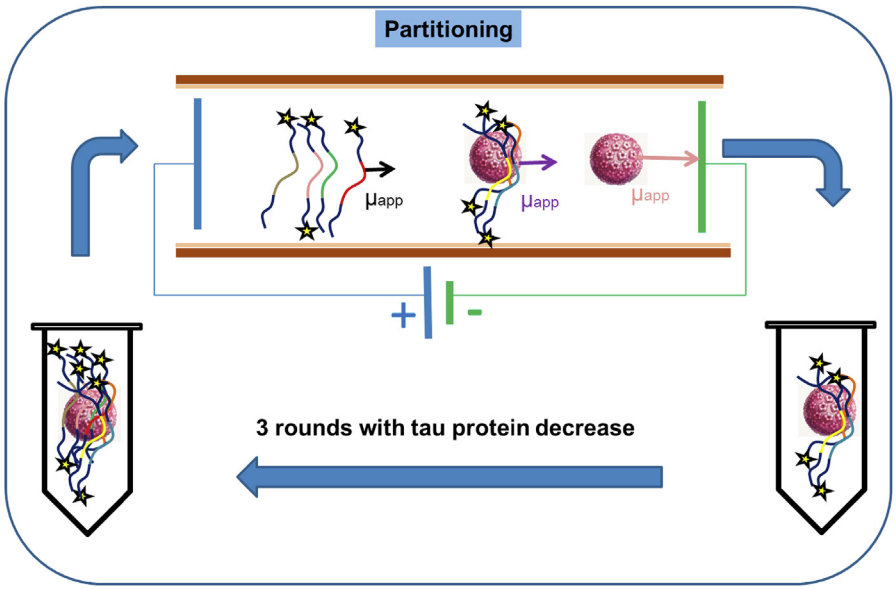

Scheme 1. Summary of non-SELEX process. Randomized library is mixed with the target and injected into the capillary tube of capillary electrophoresis (Partitioning). Low affinity ssDNA sequences are separated from high affinity ssDNA sequences because of the different electrophoretic mobility. Separation was iterated for three rounds (with no amplification in between) prior to a single amplification step by PCR. Finally aptamer candidates were recovered by gel electrophoresis (Purification).

Preliminary steps focused on the (i) determination of the aptamer collection window and (ii) definition of the best initial DNA/τ ratio. The aptamer selection by non-SELEX requires optimal electrophoretic separation between the target and the ssDNA library [29]. To this aim, we first evaluated the nucleic acid library and τ migration behavior. For the determination of the aptamer collection window, a mixture of the protein and library was injected in the capillary and was visualized using the 200 nm wavelength detector. Usually proteins are specifically detected at 280 nm wavelength (Soret's band), but τ absorbance in this UV region was very low due to the little amount of aromatic amino acid residues (low molar absorptivity coefficient of 7450 M^{-1} cm^{-1}) [30]. Protein τ migrated faster than free ssDNA due to less negative charges, with a great difference in migration time between the two species of about 20 min. As the mobility of the complex is conventionally intermediate between that of free protein and free DNA, the target-binding sequences could be easily recovered during the non-SELEX selection through a collection window that started during the τ zone and terminated ahead the DNA peak. The choice of the target concentration in the pre-incubated solution is another key point for successful selection. We initially performed experiments with an equilibrium mixture containing 750 nM of τ and 40 μM of DNA library. After injection of a plug onto the capillary, a qPCR analysis of the collected fraction was realized in order to assess the formation of the DNA-τ complex under these conditions. The C_t (threshold cycles) value obtained for the protein-containing equilibrium sample was almost identical to that of control (Fig. 1, red, dashed-dot line; blue, solid line respectively). The τ concentration in the equilibrium mixture was then 10-fold increased. This approach showed only little influence on the migration time of the species. However, the C_t value was significantly lowered as compared with the previous experimental set-up (6.26 ± 0.04 versus 17.57 ± 0.44). These operative conditions revealed the formation of a more significant amount of complex, and were then adopted as initial target concentration for the non-SELEX partitioning.

During the three rounds of the non-SELEX selection process, the τ concentration in the equilibrium mixture was diminished from 7.5 μM (round 1) to 75 nM (round 3). The affinity evolution of the

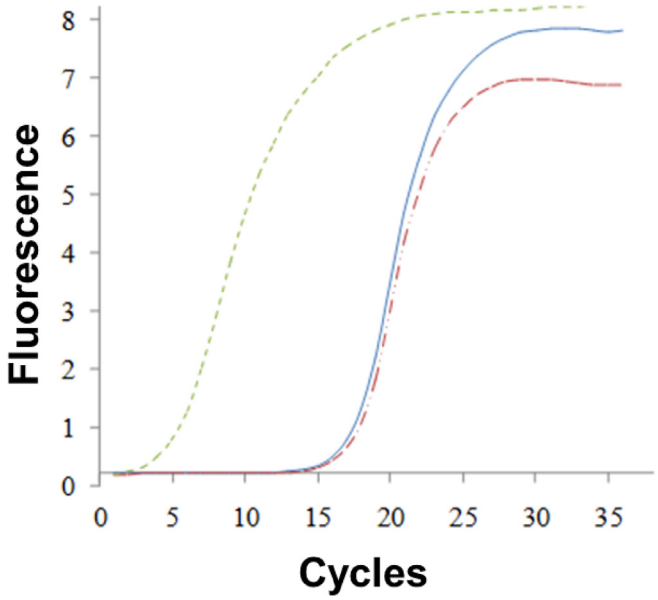

Fig. 1. Comparison of qPCR experiments realized after capillary electrophoretic separation and fraction collection in 30 μL in running buffer with 40 μM of ssDNA (library alone, blue, solid line), 40 μM of ssDNA and 750 nM τ (red, dashed-dot line), and 40 μM of ssDNA and 7.5 μM τ (green, dashed line). (For interpretation of the references to colour in this figure legend, the reader is referred to the Web version of this article.)

different pools was constantly monitored by NECEEM-based measurements. To achieve this, a portion of the collected DNA pools was first PCR amplified with fluorescently-tagged primers and UV quantitated. The resulting DNA solution (100 nM) was then mixed with a constant protein amount (3 μM), and injected into the capillary using the experimental selection conditions (except that the UV detection was replaced by a LIF detection). As can be seen in Fig. 2A, a peak was observed on the electropherogram at about 10 min. The height of this peak increased at each round, suggesting that it corresponded to an increase in the τ-DNA complex.

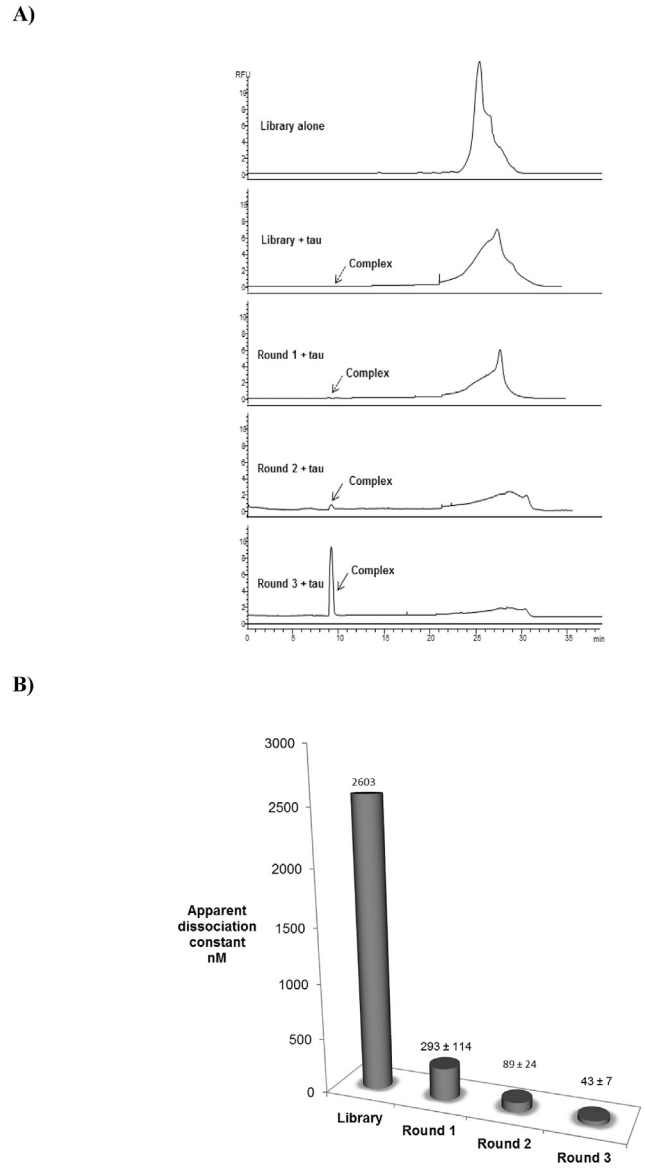

Fig. 2. a) Electropherograms of the equilibrium mixture of a known amount of target and each DNA pool collected from the three non-SELEX rounds (after PCR amplification and purification). Traces from either free library alone or mixed with the target are also presented for comparison. CE conditions are the identical to those of the non-SELEX process, but with LIF detection. b) Progress of the selection procedure assessed through the calculation of bulk K_D extracted from the electropherogram data.

Concomitantly, the free DNA peak height was diminished and it was associated to the appearance of a significant DNA part dissociated from the complex (the 'decay bridge'). The bulk affinity of DNA pools to the τ protein can be estimated through a binding analysis relying on the determination of peak areas for the complex, the free DNA and the decay bridge. Due to the large portion of the complex-dissociating DNA, a systematic method developed by Krylov and colleagues was used to reliably determine the overlap between the bridge and the DNA peak [31]. A constant reduction in the apparent dissociation constant value was reported as the number of rounds increased (Fig. 2B). The bulk affinity of the naïve library to the target was relatively weak (apparent dissociation constant > 2.5 μM), in accordance with previous results on the interaction between ssDNA and the τ protein [10]. A great improvement in the binding affinity was reached for the DNA pools from rounds 2 and 3, with a respective 30 and 60-fold decrease in the bulk dissociation constant as compared to the initial library.

3.2. Identification of non-SELEX isolated sequences

Once the non-SELEX selection was completed, we subsequently performed high-throughput sequencing of the DNA pool originating from the round 3. Ion torrent sequencing gave rise to a 2255 different sequences. Only 59% of the sequences have the expected size of 30 nucleotides while most of the others have a reduced size of a few nucleotides (Supplementary Information Fig. S1). Almost all sequences were found at one copy and about one hundred sequences were found several times with a maximum of four copies (Fig. S1B). All sequences were separated from the others with an average Levenshtein distance of about 21 and a minimum distance of 11, meaning that two sequences are separated by at least 11 mutations, deletions or insertions (Fig. S1C). This distance is very large for a random region of 30 nucleotides showing that the library is still constituted by very heterogeneous sequences, which cannot be clustered easily into families. The sequences were then analyzed using the MEME-suite software in order to identify conserved motifs. However, no highly conserved motifs were identified while the average affinity of the library was 60 times better. Such a huge diversity of affine sequences is consistent with the intrinsic nature of the non-SELEX selection that obviously alleviated the enrichment of the DNA binders because of the lack of repeated PCR amplifications. Five different sequence blocks were subsequently isolated by grouping aptamers on the basis of the predominance of some nucleotides (group 1 with a dominance of T, and a lot of C; group 2 with a dominance of T and a lot of G and C; group 3 with a dominance of T and a lot of C and A; group 4 with a dominance of G; group 5 with a dominance of C). Five oligonucleotidic sequences from each one of these groups (Table S2) were then chosen for further binding affinity investigation.

3.3. Aptamer binding evaluation by SPR

The preliminary investigation was performed by immobilizing the protein target on the chip surface for SPR experiments. By this design, a fast and effective screening of the aptamers can be performed to compare their binding capability towards the τ protein target under the same conditions. Before immobilizing the τ protein on CM5 chip, its isoelectric point was estimated by a preconcentration test. This step was aimed at identifying the pH value at which the protein is positively charged. Under this condition a strong attraction between the protein and the negatively charged dextran matrix is guaranteed, and the immobilization will proceed with the best efficiency. As displayed in Fig. S2, the best pH value was found at 4.0, giving an average signal of 3460 ± 3 Resonance Unit (RU) (n = 3). On the basis of this result, further immobilization was performed at pH 4.00 giving a shift of RU, $\Delta RU_{imm} = 1784$ (Fig. S2). The five aptamers were then singularly injected at the concentration of 1 μM. The resulting sensorgrams are reported in Fig. 3, which shows that the binding capability of aptamer 3146 was significantly higher than those of the other sequences. Therefore, aptamer 3146 was selected for the design of the FA sensing platform.

3.4. Fluorescence anisotropy (FA) sensing platform

For the detection of proteins, FA aptamer-based assays rely in most cases on a direct format. In such a case, the functional oligonucleotide is terminally labeled by a fluorophore to serve as FA probe. The signaling principle is based on the FA enhancement according to the effective mass increase of the aptamer probe upon

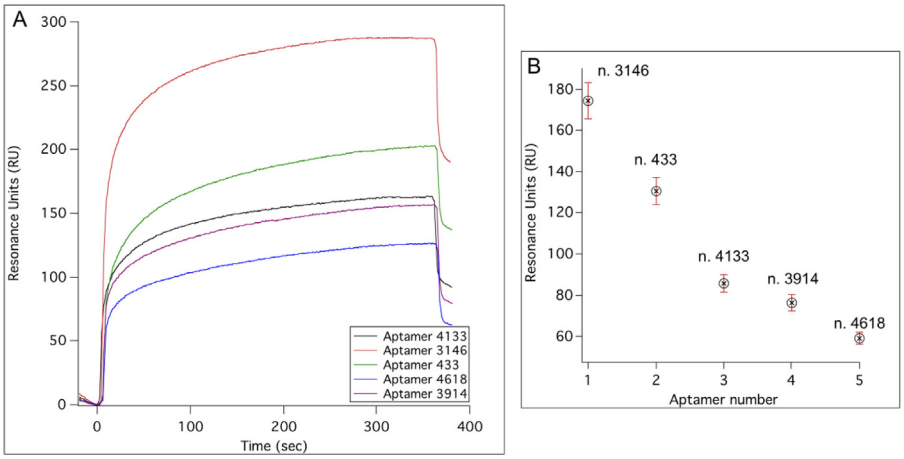

Fig. 3. SPR-based screening of binding ability of the five selected aptamers. A) binding curves recorded in real time by injecting 1 μM of each aptamer are reported superposed to evidence the relative difference; B) averaged responses in terms of SPR signals showing the highest response of that aptamer 3146 respect to the other sequences tested under the same conditions (n = 3).

complex formation with the protein [33]. In order to evaluate the selective binding features of the aptamer 3146, both the whole τ protein target and a number of isoforms (as well as the R3 peptide) were used as analytes. These isoforms range from 352 to 441 amino acids and differ from each other by the presence of either three 3R or four repeat-regions 4R (R1−R4) in the carboxy-terminal (C-terminal) part of the molecule and the absence or presence of one or two inserts (29 or 58 amino acids) in the amino-terminal (N-terminal) part (Fig. S3A) [32]. A more specifically peptide (Fig. S3B) within the repeat region corresponding to a little part of R1 and R3 peptide was also tested.

Under the binding buffer (20 mM Tris, pH 7.5; 30 mM NaCl, 5% glycerol and 1 mM $MgCl_2$) conditions, the FA signal for the fluorescein-labeled aptamer 3146 in the absence of target (r_f) was found to be relatively low for a 24 kDa species, that is comprised between 0.074 ± 0.001 and 0.086 ± 0.001 (depending on the experiment room temperature). This reduced value can be attributed to the local motional freedom of the fluorescein dye that originates from the electrostatic repulsion between the polyanionic DNA and the negatively charged fluorophore [34]. The binding of the τ proteins to the aptamer probe resulted in the increase in the FA signal (Fig. 4). Indeed, at a protein concentration comprised between 800 nM and 1000 nM, the measured FA signal reached 0.195 ± 0.000 for τ-441, 0.182 ± 0.002 for τ-381, 0.172 ± 0.001 for τ-383 and 0.179 ± 0.001 for τ-352, leading to a great FA change of about 0.100 in each case. Typically, as the result of the intense segmental motion of the DNA diffusion-uncoupled dye [35], the FA change of the fluorescein-tagged aptamer upon protein binding is of limited magnitude, no more than 0.050 [33]. Thus, the significant response observed in the present work very likely originates from not only the increase in the apparent molecular mass of the probe but also from the interaction between the fluorescein label and the τ protein that would hinder the dye local movement. Moreover, similar behavior has been previously reported by Zou et al. [36] These authors demonstrated that the aptamer-attached fluorescein can be strongly coupled to the target upon the complex formation through electrostatic interactions between the anionic label and the cationic protein, allowing a significant FA variation of about 0.120. R3 peptide did not cause any significant response over the tested concentration range. This result did not allow us to conclude on the aptamer-peptide interaction because of the low molecular mass of the peptide (2.7 kDa) which probably generated only a negligible change in the apparent mass value of the tracer. The

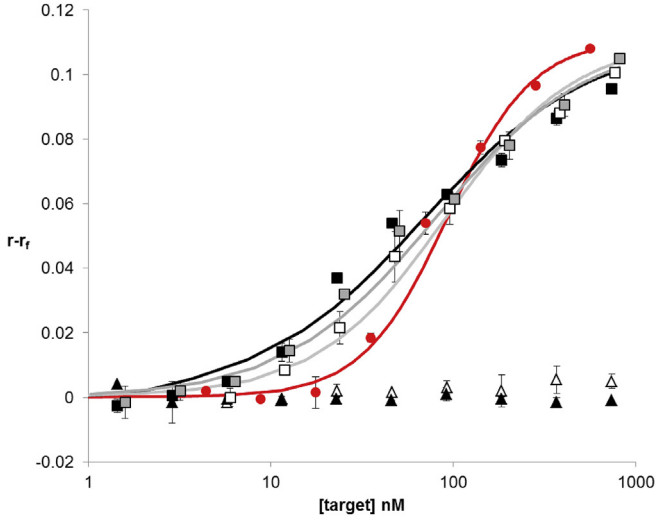

Fig. 4. Fluorescence anisotropy change of 5′-F-Aptamer 3146 with increasing τ protein 441 (red circle), 383 (white square), 381 (black square) and 352 (grey square). White and black triangle symbols represent the data for the noncognate ligand HSA and R3 peptide, respectively. The theoretical curve (–) is recreated using equation parameters (see experimental section K_D determination) obtained and adapted by fitting Eq (2) to f_b. Probe concentration = 10 nM. Binding buffer conditions: 20 mM Tris, pH 7.5; 30 mM NaCl, 5% glycerol and 1 mM $MgCl_2$. (For interpretation of the references to colour in this figure legend, the reader is referred to the Web version of this article.)

specificity of the sensing platform was further assessed by using HSA as a potential non-cognate analyte. As expected, no FA variation was observed upon addition of HSA (Fig. 4), confirming that the signal transduction is dependent on the τ binding to the aptamer 3146.

The dissociation constants for the complexes formed between the 3146 aptamer and the four isoforms of the τ protein was determined from the Hill binding model (Table 1). We noticed that the n_H values corresponding to the Hill coefficients were different for the target protein (τ-441 = 1.86 ± 0.19) as compared to the other tested τ-isoforms (τ-381 = 0.96 ± 0.05; τ-352 = 1.05 ± 0.065; τ-383 = 1.22 ± 0.07). These results highlight that the recognition mechanism of τ-381, τ-352, τ-383 should be related to a non-cooperative binding process whereas the binding of τ-441 to the aptamer relies on a positively cooperative phenomenon, with a n_H

Table 1
Dissociation constants for previously reported aptamer-protein or peptide complexes isolated from CE SELEX methods.

Proteins/Peptides	Aptamer/method	Dissociation constant	Ref
τ-441 protein	DNA/non-SELEX	13 ± 3 nM	Our work
τ-381 protein		116 ± 6 nM	
τ-352 protein		84 ± 6 nM	
τ-383 protein		49 ± 4 nM	
αC-conotoxin PrXA	DNA/CE-SELEX	120–246 nM*	[14]
HE4-GST ovarian cancer biomarker	DNA/CE-SELEX	280-750,000 nM**	[41]
Alpha-fetoprotein (AFP)	DNA/CE-SELEX	500 nM	[42]
rhVEGF165		21–164 nM**	[43]
Ara h1	DNA/CE-SELEX	353–450 nM	[44]
Leptin	DNA/CE-SELEX	320–3000 nM**	[45]
Protective antigen anthrax toxin	DNA/CE-SELEX	112–1140 nM	[46]
Cdc42-GTP	DNA/non-SELEX	600–2000 nM	[47]
PAK1		150–600 nM	
MRCKa-KD		60–130 nM	
Ricin	DNA/CE-SELEX	58–80 nM	[48]
Neuropeptide Y	DNA/CE-SELEX	1.1–11 μM	[13]
HIVRT	DNA/CE-SELEX	180–500 pM	[12]
IgE	DNA/CE-SELEX	27–73 nM	[11]
IgE	DNA/CE-SELEX	23–39 nM	[49]

*one sequence with dissociation constant higher than 5000 nM.
**Two distinct methods.

value of around 2. The microscopic dissociation constant was lower for τ-441 (13 ± 3 nM) than for τ-381, τ-352 and τ-383 (116 ± 6 nM, 84 ± 6 nM, 49 ± 4 nM respectively). The calculated values, clustered in the low-nanomolar range, are lower than most of those obtained for protein or peptide aptamers isolated by CE-SELEX (Table 1). Only one example of CE-SELEX-selected aptamer exhibits a lower dissociation constant (for HIV reverse transcriptase, ranging from 180 to 500 pM, see Table 1). It is also of interest to mention that the isolated aptamer 3146 displays about 2.25 times greater binding features than the oligonucleotide tested by Krylova and colleagues for the τ-381 isoform (dissociation constant of ~85 nM *vs* 190 nM).

The analytical features of the FA aptasensor were subsequently investigated. The estimation of the detection limit was based on the 3σ/S procedure, where σ is the standard deviation of the response in the absence of target and S the slope of the titration curve linear part. A lower detection limit was attained for τ-381 and τ-352 than for τ-383 and τ-441 (3.2 nM and 6.3 nM compared to 22 and 28 nM respectively). For the τ-381 and τ-352 isoforms, the analytical performances of the present FA assay are similar to the previously reported FA aptasensors dedicated to protein targets. For example, the limits of detections (LODs) of 1 nM, 2 nM and 4.9 nM were obtained for angiogenin [37], PDGF-BB [33] and lysozyme [36], respectively (Table 2). Finally, the τ-441 LOD was slightly higher than those we previously reported with a monoclonal antibody-based SPR biosensor (28 nM *vs* 7.8 nM) [38]. However, these achieved LODs are currently not sufficient to detect clinical levels of τ protein, which are in the pM range. Further experiments could be performed in the future to increase the FA signal and consequently the assay sensitivity, for instance by using mass-based amplification approaches as previously reported for other protein targets [39,40].

Table 2
Limits of detection for previously reported FA direct assays dedicated to protein targets.

Proteins	Aptamer DNA	Dye	Detection Limit nM	Ref
τ-441 protein	76 mer	Fluo	28	Our work
τ-381 protein	3146		3.2	
τ-352 protein			6.3	
τ-383 protein			22	
Thrombin	29 mer	TMR	0.1	[50]
	C15T-Apt		0.1	
	3′-Apt			
PDGF-BB	35 mer	Fluo	2	[33]
			0.22*	
Lysozyme	80 mer	FAM	4.9	[36]
IgE	37 mer	TR	nd	[51]
	1B**	TR	0.35	
	1C**			
Angiogenin	72 mer	Fluo	1	[52]

Fluo for fluorescein.
FAM for 6-carboxyfluorescein.
TR for Texas Red.
TMR forTetramethylrhodamine.
*With the use of a lower aptamer concentration at the 2 nM range and with a more efficient optical signal collection.
**1B and 1C, Texas Red conjugates with 8- and 14-atom dye linkers.

4. Conclusion

The choice of a non-SELEX strategy has accelerated the procedure of aptamer selection excluding repetitive steps of amplification by PCR. The bulk dissociation constant of the ssDNA library decreases from the micromolar to the nanomolar range within three rounds, demonstrating an enrichment of binders. After high-throughput sequencing, five selected aptamers have been chosen and evaluated using immobilized τ protein on a SPR chip. The most responsive aptamer (named 3146) has been used as binding element in the development of a direct FA biosensor. The calculated dissociation constant values are better (13 nM for τ-441 protein) or comparable (116 nM, 84 nM, and 49 nM for τ-381, τ-352 and τ-383 protein, respectively) to those classically obtained by CE-SELEX with aptamers directed against proteins or peptides. This study demonstrates that the aptamer 3146 could be promising as bio-recognition element in the development of aptamer-based biosensors for detecting most of the τ protein isoforms.

Acknowledgments

The authors thank the Università Italo – Francese for financial support (Cap. 3 – Vinci project). SL, MM, SS and EP would also thank the INBB consortium [comment]. SS and MM thank the Ministry of Education, University and Research (MIUR) for the scientific program SIR2014 Scientific Independence of young Researchers (RBSI1455LK).

This program is supported by a grant from the LabEx ARCANE (grants ANR-11-LABX-0015 & ANR-11-LABX-0003-01) and from Investissement d'Avenir ANR-11-INBS-0011 - NeurATRIS: A Translational Research Infrastructure for Biotherapies in Neurosciences.

Appendix A. Supplementary data

Supplementary data related to this article can be found at https://doi.org/10.1016/j.aca.2018.07.029.

References

[1] K. Blennow, H. Hampel, M. Weiner, H. Zetterberg, Nat. Rev. Neurol. 6 (2010) 131–144.
[2] S. Scarano, S. Lisi, C. Ravelet, E. Peyrin, M. Minunni, Anal. Chim. Acta 940 (2016) 21–37.
[3] C. Humpel, Trends Biotechnol. 29 (2011) 26–32.
[4] H. Vanderstichele, E. Stoops, E. Vanmechelen, A. Jeromin, Alzheimer's Res. Ther. 4 (2012) 39.
[5] A. Bouvier-Müller, F. Ducongé, Biochimie 145 (2018) 73–83.
[6] T. Kampers, P. Friedhoff, J. Biernat, E.M. Mandelkow, E. Mandelkow, FEBS Lett. 399 (1996) 344–349.
[7] J.H. Kim, E. Kim, W.H. Choi, J. Lee, J.H. Lee, H. Lee, D.E. Kim, Y.H. Suh, M.J. Lee, Mol. Pharm. 13 (2016) 2039–2048.
[8] S. Kim, A.W. Wark, H.J. Lee, Anal. Chem. 88 (2016) 7793–7799.
[9] S. Camero, M.J. Benitez, A. Barrantes, J.M. Ayuso, R. Cuadros, J. Avila, J.S. Jimenez, J Alzheimers Dis 39 (2014) 649–660.
[10] S.M. Krylova, M. Musheev, R. Nutiu, Y. Li, G. Lee, S.N. Krylov, FEBS Lett. 579 (2005) 1371–1375.
[11] S.D. Mendonsa, M.T. Bowser, J. Am. Chem. Soc. 126 (2004) 20–21.
[12] R.K. Mosing, S.D. Mendonsa, M.T. Bowser, Anal. Chem. 77 (2005) 6107–6112.
[13] S.D. Mendonsa, M.T. Bowser, J. Am. Chem. Soc. 127 (2005) 9382–9383.
[14] T. Abd El Aziz, C. Ravelet, J. Molgo, E. Fiore, S. Pale, M. Amar, S. Al Khoury, J. Dejeu, M. Fadl, M. Ronjat, G. Sotoing Taiwe, D. Servent, E. Peyrin, M. De Waard, Sci. Rep. 7 (2017) 7202.
[15] M. Berezovski, M. Musheev, A. Drabovich, S.N. Krylov, J. Am. Chem. Soc. 128 (2006) 1410–1411.
[16] X. Yu, Y. Yu, Appl. Biochem. Biotechnol. 173 (2014) 2019–2027.
[17] J. Ashley, S.F.Y. Ji, K. Fau - Li, S.F. Li, Electrophoresis 33 (2012) 2783–2789.
[18] Y. Liu, C. Wang, F. Li, S. Shen, D.L.J. Tyrrell, X.C. Le, X.-F. Li, Anal. Chem. 84 (2012) 7603–7606.
[19] D.M. Jameson, J.A. Ross, Chem. Rev. 110 (2010) 2685–2708.
[20] I. Lamberti, S. Scarano, C.L. Esposito, A. Antoccia, G. Antonini, C. Tanzarella, V. De Franciscis, M. Minunni, Methods 97 (2016) 58–68.
[21] E. Fiore, E. Dausse, H. Dubouchaud, E. Peyrin, C. Ravelet, Front. Chem. 3 (2015) 49.
[22] L.T. Cherney, M. Kanoatov, S.N. Krylov, Anal. Chem. 83 (2011) 8617–8622.
[23] M.A. Quail, M. Smith, P. Coupland, T. Otto, S. Harris, T. Connor, A. Bertoni, H. Swerdlow, Y. Gu, BMC Genom. 2012 (13) (2012) 341, 341 13.
[24] N. Nguyen Quang, G. Perret, F. Ducongé, Pharmaceuticals 9 (2016) 76.
[25] T.L. Bailey, M. Boden, F.A. Buske, M. Frith, C.E. Grant, L. Clementi, J. Ren, W.W. Li, W.S. Noble, Nucleic Acids Res. 37 (2009) W202–W208.
[26] A. Rath, M. Glibowicka, V. Nadeau, G.N. Chen, C.M. Deber, Proc. Natl. Acad. Sci. U. S. A. 106 (2009) 1760–1765.
[27] R.L. Weinberg, D.B. Veprintsev, A.R. Fersht, J. Mol. Biol. 341 (2004) 1145–1159.
[28] G.M. Wilson, Reviews in Fluorescence, New York, 2005.
[29] M.V. Berezovski, M. Musheev, A. Drabovich, J. Jitkova, S.N. Krylov, Nat. Protoc. 1 (2006) 1359–1369.
[30] Y. Furukawa, K. Kaneko, N. Nukina, J. Biol. Chem. 286 (2011) 27236–27246.
[31] M. Kanoatov, S. Mehrabanfar, S.N. Krylov, Anal. Chem. 88 (2015) 9300–9308.
[32] L. Buée, T. Bussière, V. Buée-Scherrer, A. Delacourte, P.R. Hof, Brain Res. Rev. 33 (2000) 95–130.
[33] X. Fang, T. Cao, Z. Fau - Beck, W. Beck, T. Fau - Tan, W. Tan, Anal. Chem. 73 (2001) 5752–5757.
[34] J.R. Unruh, G. Gokulrangan, G.H. Lushington, C.K. Johnson, G.S. Wilson, Biophys. J. 88 (2005) 3455–3465.
[35] H. Huang, H. Wei, M. Zou, X. Xu, B. Xia, F. Liu, N. Li, Anal. Chem. 87 (2015) 2748–2754.
[36] M. Zou, Y. Chen, X. Xu, H. Huang, F. Liu, N. Li, Biosens. Bioelectron. 32 (2012) 148–154.
[37] Z. Wang, D. Wilkop, T. Fau - Xu, Y. Xu, D. Fau - Dong, G. Dong, Y. Fau - Ma, Q. Ma, G. Fau - Cheng, Q. Cheng, Anal. Bioanal. Chem. 389 (2007) 819–825.
[38] S. Lisi, S. Scarano, S. Fedeli, E. Pascale, S. Cicchi, C. Ravelet, E. Peyrin, M. Minunni, Biosens. Bioelectron. 93 (2017) 289–292.
[39] C.H. Lu, C.-L. Yang, Hh Fau - Zhu, X. Zhu, Cl Fau - Chen, G.-N. Chen, X. Fau - Chen, G.N. Chen, Angew. Chem. Int. Ed. 48 (2009) 4785–4787.
[40] L. Kang, B. Yang, X. Zhang, L. Cui, H. Meng, L. Mei, C. Wu, S. Ren, W. Tan, Anal. Chim. Acta 879 (2015) 91–96.
[41] R.M. Eaton, J.A. Shallcross, L.E. Mael, K.S. Mears, L. Minkoff, D.J. Scoville, R.J. Whelan, Anal. Bioanal. Chem. 407 (2015) 6965–6973.
[42] L. Dong, Q. Tan, W. Ye, D. Liu, H. Chen, H. Hu, D. Wen, Y. Liu, Y. Cao, J. Kang, J. Fan, W. Guo, W. Wu, Sci. Rep. 26 (2015) 15552.
[43] M. Jing, M.T. Bowser, Anal. Chem. 85 (2013) 10761–10770.
[44] D.T. Tran, K. Knez, K.P. Janssen, J. Pollet, D. Spasic, J. Lammertyn, Biosens. Bioelectron. 43 (2013) 245–251.
[45] J. Ashley, S.F.Y. Li, Anal. Biochem. 434 (2013) 146–152.
[46] L.N. Cella, P. Sanchez, W. Zhong, N.V. Myung, W. Chen, A. Mulchandani, Anal. Chem. 82 (2010) 2042–2047.
[47] J. Tok, J. Lai, T. Leung, S.F.Y. Li, Electrophoresis 31 (2010) 2055–2062.
[48] J. Tang, J. Xie, N. Shao, Y. Yan, Electrophoresis 27 (2006) 1303.
[49] S.D. Mendonsa, M.T. Bowser, Anal. Chem. 76 (2004) 5387–5392.
[50] D. Zhang, Q. Zhao, B. Zhao, H. Wang, Anal. Chem. 84 (2012) 3070–3074.
[51] G. Gokulrangan, J.R. Unruh, D.F. Holub, B. Ingram, C.K. Johnson, G.S. Wilson, Anal. Chem. 77 (2005) 1963–1970.
[52] W. Li, K. Wang, W. Tan, C. Ma, X. Yang, Analyst 132 (2007) 107–113.